



You have downloaded a document from
RE-BUŚ
repository of the University of Silesia in Katowice

Title: Influence of crystallographic orientation on creep resistance of single-crystal superalloy

Author: Barbara Kościelniak, Kamil Gancarczyk, Marek Poręba, Robert Albrecht

Citation style: Kościelniak Barbara, Gancarczyk Kamil, Poręba Marek, Albrecht Robert. (2020). Influence of crystallographic orientation on creep resistance of single-crystal superalloy. "Advances in Manufacturing Science and Technology" (2020), nr 3, s. 93-98. DOI: 10.2478/amst-2019-0017



Uznanie autorstwa - Użycie niekomercyjne - Bez utworów zależnych Polska - Licencja ta zezwala na rozpowszechnianie, przedstawianie i wykonywanie utworu jedynie w celach niekomercyjnych oraz pod warunkiem zachowania go w oryginalnej postaci (nie tworzenia utworów zależnych).



UNIwersYTET ŚLĄSKI
W KATOWICACH



Biblioteka
Uniwersytetu Śląskiego



Ministerstwo Nauki
i Szkolnictwa Wyższego

Influence of Crystallographic Orientation on Creep Resistance of Single-Crystal Superalloy

Barbara Kościelniak^{1,*}, Kamil Gancarczyk¹, Marek Poręba¹, Robert Albrecht²

¹Department of Materials Science, Faculty of Mechanical Engineering and Aeronautics, Rzeszow University of Technology, Rzeszow, Poland

²Institute of Materials Science, University of Silesia, Chorzow, Poland

Abstract

This paper focuses on the influence of crystallographic orientation on creep resistance of CMSX-4 nickel-based superalloy. The single-crystal rods of CMSX-4 superalloy were manufactured with the use of the Bridgman method at a withdrawal rate of 3 mm/min. The crystallographic orientation of the rods was determined by the X-ray Ω -scan method with OD-EFG diffractometer and the Laue back-reflection technique. The creep tests were performed at a temperature of 982°C and the value of stress $\sigma = 248$ MPa. Microstructural investigation before and after the creep test of CMSX-4 superalloy was performed using a scanning electron microscope. The results showed that the distribution of the values of a angle strongly affects the creep resistance of a single-crystal superalloy.

Keywords

CMSX-4 superalloy, creep resistance, crystal orientation, microstructure

1. Introduction

The high-pressure turbine blades are the elements of a turbojet engine critical for flight safety. These parts are exposed to high temperatures, high static and variable stresses, and strong cyclic thermal loads during their operation. Hence, they should be characterized by very good mechanical properties, especially high creep resistance at a temperature below 1,170 °C. The single-crystal nickel-based superalloys are used for the production of high-pressure turbine blades. Elimination of grain boundaries in single-crystal superalloys reduces the creep rate leading to an increase in the time of safe operation of the turbojet engine. Grain boundaries provide high diffusivity paths for vacancies during creep. Therefore, the elimination of grain boundaries has reduced grain boundary cavitation and cracking, resulting in significantly enhanced creep ductility [1–6].

Moreover, another important factor that determines the creep resistance of turbine blade is crystallographic orientation of a single crystal. The high creep strength of turbine blade requires that the direction of single-crystal withdrawal should be parallel or slightly deviated from [001] crystallographic direction (deviation angle α) (Figure 1). The high deviation angle of single-crystal casting leads to a decrease in its mechanical properties in longitudinal direction. Therefore, it is usually assumed that the value of the deviation angle α should be lower than 15° [1, 7–14].

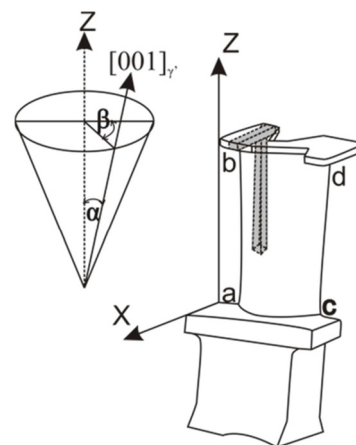


Figure 1. Deviation angle α between the direction of single-crystal withdrawal and [001] crystallographic direction [15].

The modern method of measurement of the deviation angle α , which was developed as an alternative to the Laue back-reflection technique, is X-ray (Ω -scan method). Using a conventional X-ray source, the Ω -scan method gives more precise results for the crystal orientation of castings made from single-crystal superalloys [9, 16, 17]. In this study, the W-scan method was used to determine the value of the deviation angle α of single crystal made from commercial CMSX-4 nickel-based superalloy in the as-cast state. As well, the Laue back-reflection technique was applied for comparison. Furthermore, another purpose of the work was to evaluate the influence of the value

* Corresponding author: Barbara Kościelniak
E-mail: b.koscielnia@prz.edu.pl

of deviation angle α on creep behavior of single-crystal superalloy. In addition, the microstructural changes of the CMSX-4 superalloy after creep rupture are also described in this paper.

2. Material and Methods

Three single-crystal rods (I, II, and III) in the as-cast state made from CMSX-4 nickel-based superalloy (Table 1) were used in the experiment. The rods were obtained by the directional solidification process using the Bridgman method in a vacuum furnace ALD VIM-IC 2 E/DS/S.C. The withdrawal rate of single crystal from the furnace was 3 mm/min. The manufacturing process was performed in the R&D Laboratory for Aerospace Materials of Rzeszow University of Technology.

Specimens were prepared from two fragments of single-crystal rods (A and B specimens), which were cut along the direction of their withdrawal (Figure 2).

Specimen A was used to determine the values of deviation angle α of single-crystal rods in different places on the surface parallel to the direction of withdrawal. The values of deviation angle α of specimen A were determined by the X-ray W-scan method with OD-EFG diffractometer. The crystallographic orientation and values of deviation angle

α on a surface perpendicular to the direction of withdrawal (specimen B) were determined using Laue back-reflection technique. The Laue X-ray diffraction was performed at the University of Silesia using X-ray diffractometer EFG XRT-100. The values of deviation angle α of both specimens (A and B) were determined before the creep test. Evaluation of creep resistance of single-crystal rods was carried out at a temperature of 982 °C and stress $s = 248$ MPa in air, according to the ASTM E139 standard [18].

The creep test was performed using a Walter + Bai AG LFMZ—30 kN testing machine. The samples for creep tests were made from specimen A of single-crystal rods. Before and after the creep test, the microstructure of CMSX-4 superalloy was characterized using Hitachi S-3400N scanning electron microscope (SEM). The microstructure of the superalloy was revealed by chemical etching in 3 g MoO₃ + 100 mL HNO₃ + 100 mL HCl + 100 mL H₂O reagent.

3. Results and Discussion

Mapping of the values of deviation angle α of three single-crystal rods on the surface parallel to the direction of withdrawal is shown in Figure 3, and extreme values of α angle for three rods are presented in Table 2. It was found that the values of angle α measured in different places on the parallel surface of

Table 1. The chemical composition of CMSX-4 single-crystal superalloy

Element content, wt.%									
Cr	Co	Mo	W	Ta	Al	Ti	Hf	Re	Ni
6.5	9	0.6	6	6.5	5.6	1	0.1	3	bal.

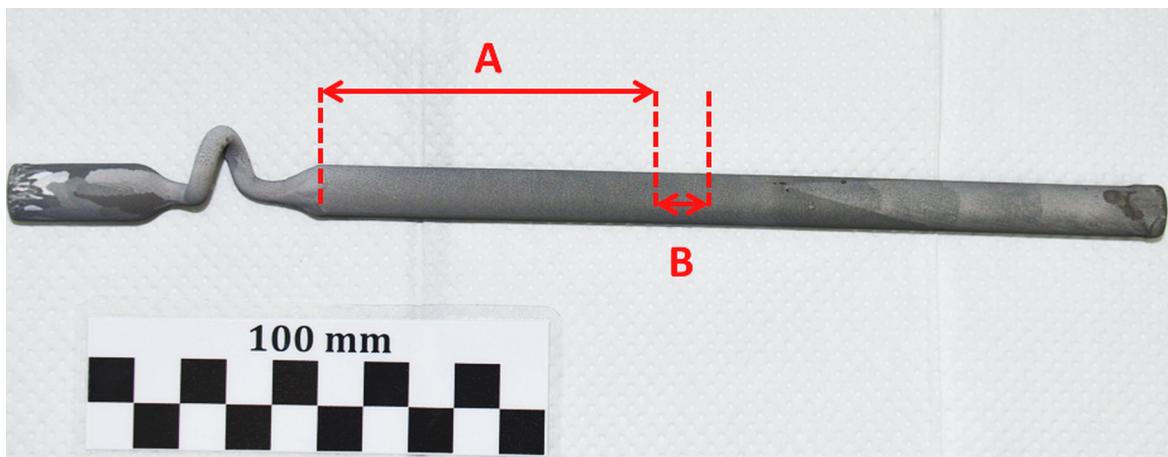


Figure 2. The sampling points of single-crystal rods made of CMSX-4 superalloy.

rods show some scatter for all tested specimens. The smallest values of angle $\alpha = 10.7^\circ$, 14.1° were measured for rod III, while the highest values of angle $\alpha = 27.1^\circ$, 28.4° were measured for rod I. Furthermore, rod III is characterized by the biggest spread of values of deviation angle α between [001] direction and withdrawal direction of the rod (Table 2). However, it can also be observed that the values of α angle in rod III changed evenly along the length of the rod—from the smallest value ($\alpha = 14.1^\circ$) to the highest ($\alpha = 10.7^\circ$). In the case of rod I, the microvolumes were observed with large differences in values of α angle. The most homogeneous distribution of values of α angle was determined in rod I (Figure 3).

To compare the results obtained from the W-scan method, the Laue X-ray diffraction was performed on a flat surface of specimen B, which was cut from the tested rods (Figure 2).

The results obtained using the W-scan method and Laue X-ray diffraction were comparable. The Laue method confirmed that rod III is characterized by the smallest value of α angle (Table 3). The crystallographic orientation of the tested rods was also determined by the Laue method. The rods II and III were characterized by [001] crystallographic direction, whereas rod I has main crystallographic direction [011] (Table 3 and Figure 4).

The tested rods made of CMSX-4 superalloy demonstrate a substantial degree of creep properties anisotropy at a temperature of 982°C and stress of 248 MPa (Figure 5).

Rod I had the longest time to rupture $t = 133.5\text{ h}$. However, rod III has been characterized by the highest creep strain at rupture $\epsilon = 33.7\%$. The crystallographic orientation studies show that the creep anisotropy existed between the two

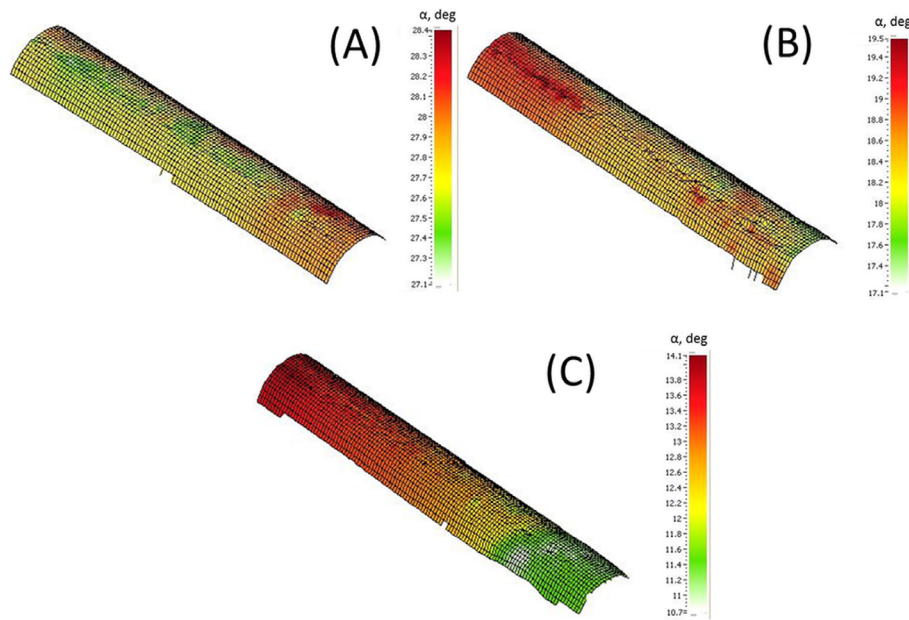


Figure 3. The values of α angle on the parallel surface of the tested rods made of CMSX-4 superalloy (specimen A): (a) rod I, (b) rod II, and (c) rod III.

Table 2. The values of deviation angle α determined by the X-ray Ω -scan method

rod I			rod II			rod III		
Min (deg)	Max (deg)	Δ (deg)	Min (deg)	Max (deg)	Δ (deg)	Min (deg)	Max (deg)	Δ (deg)
27.1	28.4	1.3	17.1	19.5	2.4	10.7	14.1	3.4

Table 3. The results of crystallographic orientation measurements carried out by the X-ray Laue back-reflection method.

	rod I	rod II	rod III
Main crystallographic direction	[011]	[001]	[001]
Deviation angle α , deg	30.5	15.9	11.8

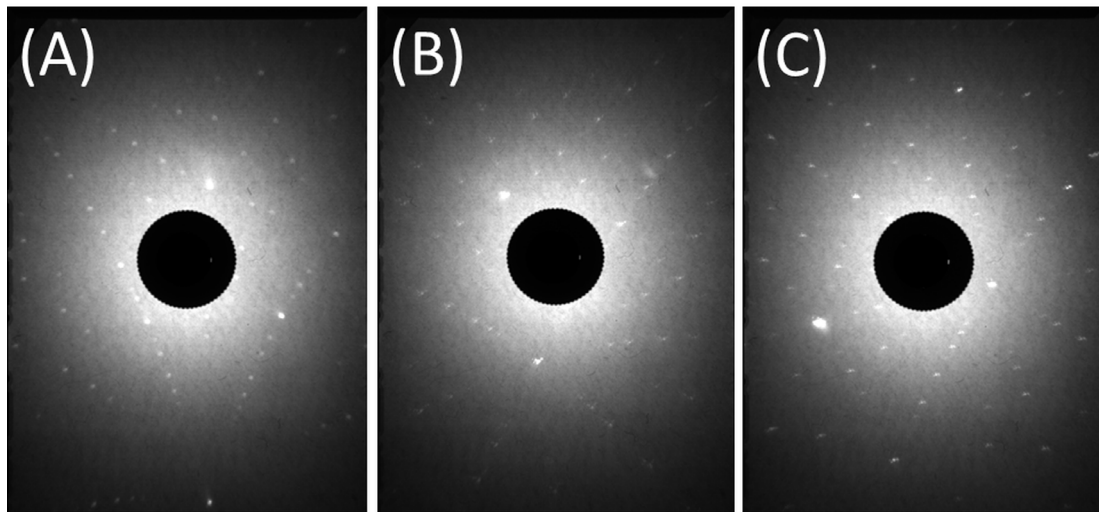


Figure 4. The images of Laue diffraction on a flat surface of tested rods made of CMSX-4 superalloy (specimen B): (a) rod I, (b) rod II, and (c) rod III.

crystallographic directions [011] and [001] (Table 3). Rod I with [011] crystallographic orientation presents the superior time to creep rupture. However, the highest deformation during creep has been measured in rod III, which has crystallographic orientation [001]. From creep resistance, the ranking of crystallographic orientation for CMSX-4 superalloy is [111], [001], and [011] and depends on the temperature and the applied stress. Besides, the creep anisotropy can be attributed to different configurations of dislocation and the orientation dependence of the misfit and external stresses [19]. Probably, this creep anisotropy in tested rods does depend not only on the direction of crystal growth but also on distribution and difference in values of α angle.

The results of the SEM investigation of CMSX-4 superalloys before and after the creep test are shown in Figures 6 and 7. The microstructure of tested rods in the as-cast state consists of g' phase precipitates in g matrix and ($g + g'$) eutectic in interdendritic areas (Figure 6).

The microstructure of CMSX-4 during creep deformation at a temperature below 950 °C undergoes three distinct stages of degradation: (i) coarsening of cuboidal precipitates of g' phase, (ii) formation of transient type of microstructure composed of rafted and coarsened precipitates of g' phase, and (iii) increase of fully rafted microstructure of superalloy. However, the coarsening of g' precipitates and the increase of rafted microstructure are not homogeneous within the microstructure. The formation of spontaneous rafts is faster within the dendrite area than in the interdendritic area [20].

After the creep test, the microstructure of all single-crystal rods is completely rafted and somewhat coarsened (Figure 7). The rafts of g' phase are long and always oriented

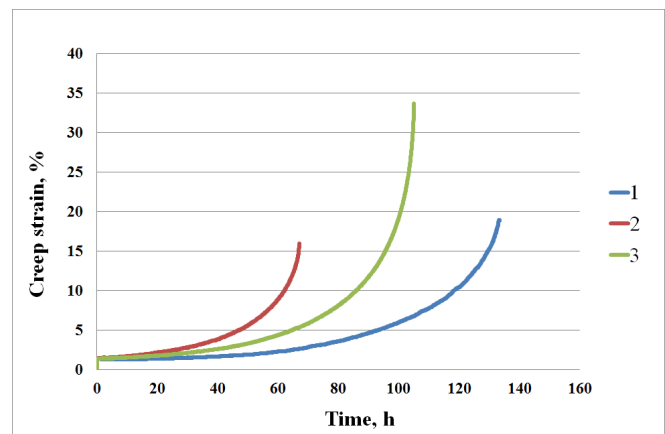


Figure 5. Creep behavior of three single-crystal rods of CMSX-4 at 982 °C/248 MPa.

perpendicular to the axis of the specimen (N-type rafting).

A large number of internal cracks were observed in the failed specimens below the fracture surface and a perpendicular direction to the fracture surface. The cracks were also formed in the interdendritic area (Figure 7). In the as-cast state of superalloy, porosity was also observed in the interdendritic area. Therefore, it is possible that cracks nucleated at pores. The propagation of cracks can be caused by the coalescence of creep-induced voids and casting pores. However, a significant difference in the amount of porosity in the tested rods before the creep test has not been observed during SEM investigation. After the creep test, the highest number of cracks was observed in rod II and the lowest number of cracks in rod I.

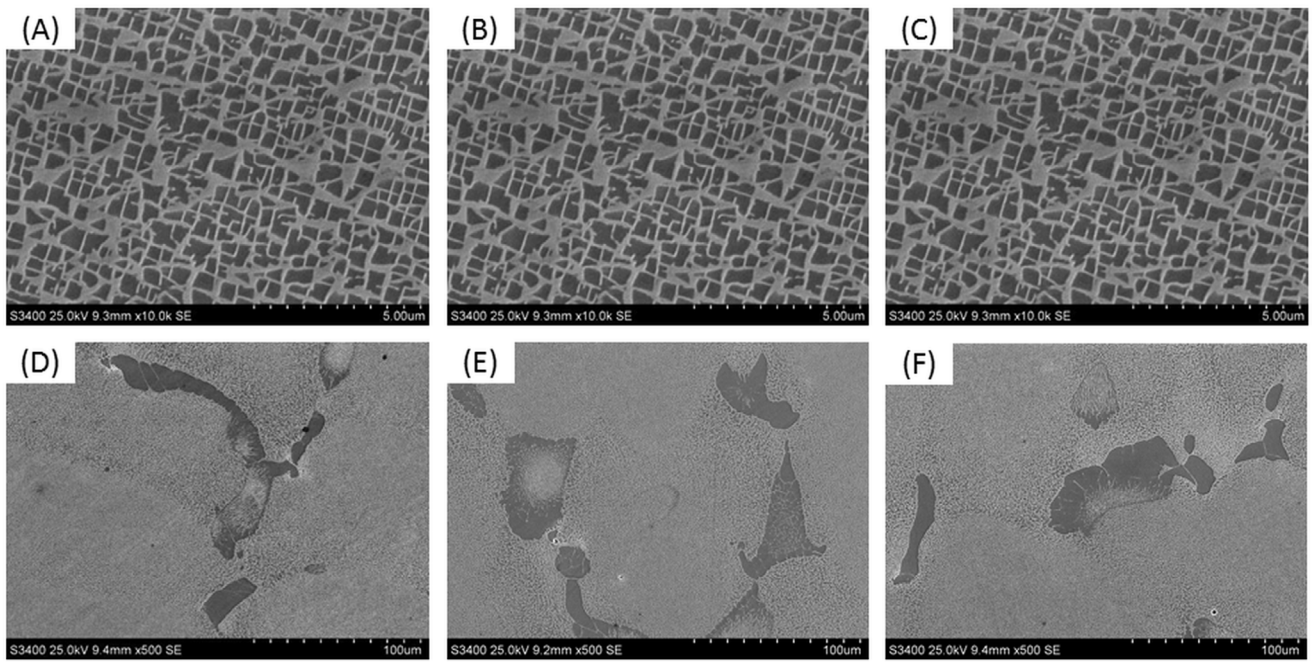


Figure 6. The SEM images of the microstructure of dendrite (a–c) and interdendritic areas (d–f) of tested rods made of CMSX-4 superalloy before creep test: (a, d) rod I; (b, e) rod II; and (d, f) rod III.

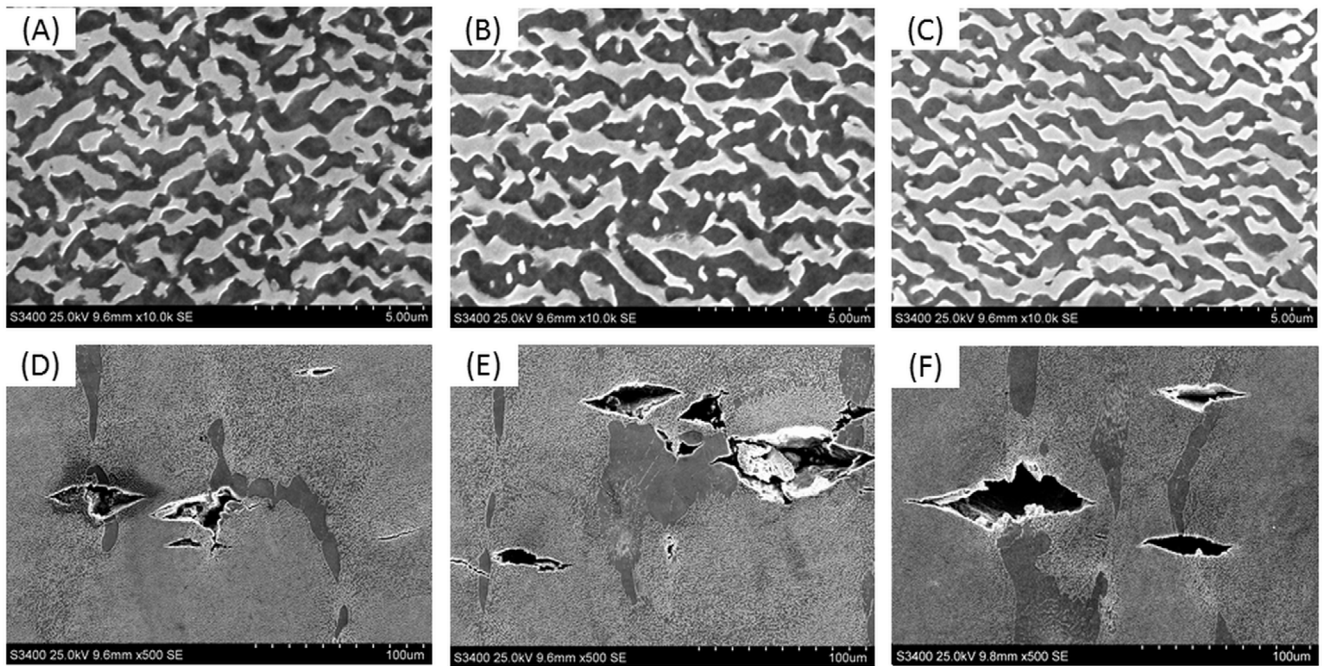


Figure 7. The SEM images of the microstructure of dendrite (a–c) and interdendritic areas (d–f) of tested rods made of CMSX-4 superalloy after creep test: (a, d) rod I; (b, e) rod II; and (d, f) rod III.

4. Conclusion

The analysis of measurement results obtained by the W-scan method and Laue X-ray diffraction showed a significant effect of the character of the distribution of values of deviation angle α on creep resistance of single-crystal CMSX-4 superalloy. It was found that the homogeneous distribution of the value of α angle on the surface parallel to the direction of withdrawal increased the time to creep rupture. The rod I exhibited the most homogeneous distribution of values of α angle, but with a much higher value of α angle, and a long time to rupture. Therefore, it can be concluded that the presence of areas with a large difference in the values of angle α reduces the creep resistance of the single-crystal superalloy (rod II). Moreover, the rod III was characterized by [011] crystallographic orientation, whereas the rest of the rods had main crystallographic orientation [001]. Therefore, the distribution of the values of α angle has a greater impact on creep behavior of single-crystal superalloy than the value of α angle or the direction of crystal growth.

The SEM investigation of rods shows that the microstructure of CMSX-4 superalloys has been changed during creep deformation. The g' phase has been perpendicularly rafted to the axis of samples (N-type rafting). Moreover, the internal cracks are also formed in the failed specimens. The lowest amount of internal cracks was observed in rod I, which was characterized by the most homogeneous distribution of values of angle α .

Acknowledgment

This work was supported by the National Science Centre Poland (NCN) under Grant No. Preludium-UMO-2016/21/N/ST8/00240.

References

- [1] R.C. REED: The superalloys fundamentals and application, Cambridge University Press, Cambridge 2006.
- [2] M.J. DONACHIE: Superalloys: a technical guide, ASM International, 2002.
- [3] M.T. POLLOCK, S. TIN: Nickel-based superalloys for advanced turbine engines: Chemistry, microstructure and properties. *J. Propul. Power.*, **22**(2006)2, 361–374.
- [4] H. ZHANG, Q. XU: Simulation and experimental studies on grain selection and structure design of the spiral selector for casting single crystal Ni-based superalloy. *Materials*, **10**(2017)11, 1236.
- [5] M. LAMM, R. SINGER: The effect of casting conditions on the high-cycle fatigue properties of the single-crystal nickel-base superalloy PWA 1483. *Metall. Mater. Trans.*, **6**(2007)38, 1177–1183.
- [6] J.B. LE GRAVEREND, et al.: Creep of a nickel-based single-crystal superalloy during very high-temperature jumps followed by synchrotron X-ray diffraction. *Acta Mater.*, **84**(2015), 65–79.
- [7] S. SEO, et al.: A comparative study of the γ/γ' eutectic evolution during the solidification of Ni-base superalloys. *Metall. Mater. Trans.*, **10**(2011)42, 3150–3159.
- [8] K. KUBIAK, et al.: Influence of manufacture conditions of the properties of CMSX-4 single crystal castings. *Mater. Eng.*, **3**(2010)31, 622–624.
- [9] K. GANCARCZYK, et al.: Determination of crystal orientation by Ω -scan method in nickel-based single-crystal turbine blades. *Metall. Mat. Trans. A*, **48**(2017)11, 5200–5205.
- [10] R.C. REED, et al.: Creep of CMSX-4 superalloy single crystals: effects of rafting at high temperature. *Acta Mater.*, **47**(1999)12, 3367–3381.
- [11] D.M. KNOWLES, D.W. HUNT: The influence of microstructure and environment on the crack growth behavior of powder metallurgy nickel superalloy RR1000. *Metall. Mat. Trans. A*, **33**(2002)10, 3165–3172.
- [12] D.W. MACLACHLAN, G.S.K. GUNTURI, D.M. KNOWLES: Modelling the uniaxial creep anisotropy of nickel base single crystal superalloys CMSX-4 and RR2000 at 1023 K using a slip system based finite element approach. *Comput. Mater. Sci.*, **25**(2002)1, 129–141.
- [13] R. ALBRECHT, et al.: Effect of creep on crystallographic orientation in single crystal superalloy. *Acta Phys. Pol.*, **4**(2016)130, 1094–1096.
- [14] X. GUO, H. FU, J. SUN: Influence of solid/liquid interfaces on the microstructure and stress-rupture life of the single-crystal nickel-base superalloy NASAIR 100. *Metall. Mater. Trans.*, **4**(1997)28, 997–1009.
- [15] W. BOGDANOWICZ, et al.: Characterization of single-crystal turbine blades by X-ray diffraction methods. *Solid State Phenom.*, **203-204**(2013), 63–66.
- [16] H. BERGER: X-ray orientation determination of single crystals by means of the Omega-scan method. *J. Phys. Arch.*, **4**(2004)118, 37–42.
- [17] H. BERGER, H.A. BRADACZEK, H. BRADACZEK: Omega-scan: an X-ray tool for the characterization of crystal properties. *J. Mater. Sci. Mater. Electron.*, **1**(2008)19, 351–355.
- [18] ASTM E139-11: Standard test methods for conducting creep, creep-rupture and stress-rupture tests of metallic materials. ASTM International, West Conshohocken, PA 2011.
- [19] P. LUKÁŠ, et al.: Creep resistance of single crystal superalloys CMSX-4 and CM186LC. *Kovove Mater.*, **43**(2005), 5–19.
- [20] J. LAPIN, et al.: The effect of creep exposure on microstructure stability and tensile properties of single crystal nickel based superalloy CMSX-4. *Kovove Mater.*, **50**(2012), 379–386.
- [21] D. SZELIGA, et al.: Temperature distribution in single crystal cast made of CMSX-4 nickel superalloy manufactured by Bridgman method. *Mater. Eng.*, **1**(2013)34, 7–13.